Fine-grained alignment of cortical signals to smartphone touchscreen temporal pattern

Wenyu Wan[1,2*], Arko Ghosh[1*]

[1]Cognitive Psychology Unit, Institute of Psychology, Leiden University, The Netherlands

[2]Department of Psychology, University of Amsterdam, The Netherlands

*Corresponding authors:

Wenyu Wan & Arko Ghosh

Institute of Psychology

Leiden University Wassenaarseweg 52

Leiden, 2333 AK, the Netherlands.

Email: w.wan@fsw.leidenuniv.nl [Wenyu Wan]

Email: a.ghosh@fsw.leidenuniv.nl [Arko Ghosh]

Abstract

Smartphone use varies ranging from rapid, rhythmic tapping (e.g., texting) to slower, irregular scrolling (e.g., browsing), resulting in diverse temporal patterns of inter-touch intervals. The underlying brain processes may dynamically align to these behaviors. We investigated population neural signals captured by using EEG during hour long smartphone use sessions (n = 53 subjects, accumulating 136869 interactions). We grouped the brain signals according to the transition patterns between consecutive touchscreen intervals (next-interval statistics), resulting in a matrix of EEG signals. Using data-driven dimensionality reduction on this matrix, we identified low-dimensional neuro-behavioral clusters that captured brain signal features associated with specific next-interval statistics. These neuro-behavioral clusters were found for diverse cortical locations spanning occipital, parietal and frontal cortices, suggesting a cortex-wide alignment to the next-interval statistics. Notably, these clusters were observed predominantly before rather than after the touchscreen interactions and they varied across individuals, suggesting personalized strategies for planning and executing smartphone use. Our findings indicate that the brain tracks and adapts to the fine-grained temporal patterns in touchscreen behavior, likely to support efficient smartphone interactions. More broadly, this work demonstrates how naturalistic smartphone use can reveal dynamic, individualized cortical adaptations to real-world temporal structure.

Keywords: smartphone behavior, temporal pattern, neuro-behavioral clusters

Introduction

The brain generates a rich repertoire of behavior in the real world, distinct from the designed tasks typically used to probe brain function (Box-Steffensmeier et al., 2022; Cisek & Green, 2024; Krakauer et al., 2017; Miller et al., 2022). The ubiquitous use of smartphones in daily life and the built-in sensors offer a fresh opportunity to close this gap (Balerna & Ghosh, 2018; Gindrat et al., 2015; Kock et al., 2023; Martin et al., 2022; van de Ruit & Ghosh, 2022). An emerging idea from the study of smartphone touchscreen interactions is that the underlying neural and behavioral processes are organized according to the intervals between touches (Balerna & Ghosh, 2018; Ceolini, Brunner, et al., 2022; Ceolini & Ghosh, 2023; Ceolini, Kock, et al., 2022; Kock & Ghosh, 2024; van de Ruit & Ghosh, 2022). For instance, the frontal theta EEG activity is correlated to the momentary rate of smartphone touches (van de Ruit & Ghosh, 2022). More specifically, the temporal pattern of inter-touch intervals - how one interval follows another - is associated with a broad range of neural and behavioral phenomena, including cortical epileptiform discharges and aging (Ceolini, Brunner, et al., 2022; Duckrow et al., 2021).

The idea underlying the smartphone next-interval statistics is that continuous smartphone touchscreen interactions can be characterized by the temporal relationship between the successive intervals (Ceolini et al., 2024; Duckrow et al., 2021). For instance, short consecutive smartphone intervals say while texting a message can be distinguished from the long consecutive intervals say while reading through news. These next-interval statistics can be captured by using the joint-interval distribution (JID), where each two-dimensional bin represents a distinct next-interval property (see explanatory scheme in Fig. 2). There is a growing body work – in disease and health – that has linked the smartphone JID to neural and behavioral processes (Ceolini, Brunner, et al., 2022; Ceolini & Ghosh, 2023; Ceolini, Kock, et al., 2022; Ceolini et al., 2024; Duckrow et al., 2021; van Nieuw Amerongen et al., 2024). In disease, cortical epileptiform discharges are associated with clusters of two-dimensional bins distributed across the smartphone JID space, but medication and seizures reduce the probability of clusters involving short consecutive intervals (van Nieuw Amerongen et al., 2024). In healthy aging, as people get older, there is a decline in the probability of clusters involving short consecutive intervals but an increase in clusters involving long consecutive intervals (Ceolini, Kock, et al., 2022). Notably, inter-individual performance differences in cognitive tasks probing sensorimotor processing are reflected in the short consecutive intervals while executive functions are reflected in a broader array of two-dimensional bins including the long intervals (Ceolini, Kock, et al., 2022). These observations where smartphone interactions with similar next interval statistics show common correlates raise the possibility that the nature of brain processing systematically varies according to the smartphone next-interval statistics.

Conventional paradigms offer some clues into how brain processing is shaped by simple interval statistics. There may be a network of processes distributed across the brain to track interval durations (Bueti et al., 2012; Karmarkar & Buonomano, 2007; Paton & Buonomano, 2018). Even in tasks targeting only one modality, these networks can span multiple brain areas (Bueti et al., 2012; Buonomano & Laje, 2010; Goel & Buonomano, 2014). For instance, in monkeys, the neurons in distinct locations including the somatosensory and prefrontal cortices are engaged in perceptual tasks to identify tactile intervals of different durations (Hernández et al., 2010; Machens et al., 2005). We recently extended this line of research to more complex tactile input trains – where consecutive tactile stimuli were distributed using a range of intervals spanning 100 ms to 10 s – to discover that the cortical tactile processing varies according the next interval statistics (Wan et al., 2024). Across studies spanning different modalities and tasks, there are indications of a rough separation of brain processes engaged in sub-second vs. supra-second behaviors (Koch et al., 2009; Lewis & Miall, 2003; Paton & Buonomano, 2018; Petter et al., 2016). In contrast to these paradigms, smartphone behavior is multi-modal,

involves distributed brain processes, and the smartphone touchscreen intervals are highly variable forming heavy tailed distributions (Kock et al., 2023; Pfister & Ghosh, 2020). It is not clear how the ideas stemming from the study of the simple tasks extend to the more complex interval statistics captured on the smartphone.

Uncovering the distributed brain processes that track the complex next-interval statistics of smartphone touchscreen touches presents some analytical challenges. EEG signals time-locked to touchscreen interactions reveal widespread activity across the scalp, suggesting the involvement of diverse neural processes surrounding a touchscreen interaction (Kock et al., 2023). These scalp signals can be decomposed into putatively distinct sources using Independent Component Analysis (ICA), with each decomposed component putatively reflecting distinct population process (Onton et al., 2006; Wessel & Aron, 2017; Wessel et al., 2016). For each source-separated brain process, and using the signals from a fixed period around smartphone interaction, we can derive a matrix of T (latencies) $\times$ I (smartphone interactions). Time-varying neural signal features may be distributed across this matrix and the signal feature may vary depending on the next-interval statistics of the touchscreen touches. To identify these patterns, Non-negative Matrix Factorization (NNMF) can be used to identify prototypical neuro-behavioral clusters, capturing time-varying neural features that occur at different levels surrounding one smartphone touchscreen interaction to the next. While this data-driven dimensionality reduction has its roots in image processing, recent work has extended it to neural and behavioral signals to explore natural stimuli processing and smartphone multi-day behavioral rhythms (Ceolini & Ghosh, 2023; Lee & Seung, 1999; Liu et al., 2017; Lu & Yin, 2015).

In this study we recorded the timing of smartphone touchscreen interactions and EEG signals while participants freely interacted with their personal smartphone for about one and a half hours. We separated the rich behavior according to the next-interval statistic using a JID of the interval spanning ~100 ms to ~10 s represented in 900 two-dimensional bins (30 x 30 bins). Independent component analysis (ICA) of the EEG signals was used to separate the putative sources as distinct brain process. We then extracted the prototypical neuro-behavioral clusters which captured the neural signal patterns and their corresponding distribution of smartphone touchscreen interaction across the temporal dynamics captured in the JID. Within each cluster, adjacent two-dimensional behavioral bins shared similar brain signal features. Our analysis was conducted at the individual level and virtually all individuals showed at least one brain process with one or more neuro-behavioral clusters showing significant 2D temporal autocorrelation. Furthermore, we find evidence for a distribution of brain processes – at different latencies from the touch and EEG signal sources – aligned to smartphone next-interval statistics.

Result

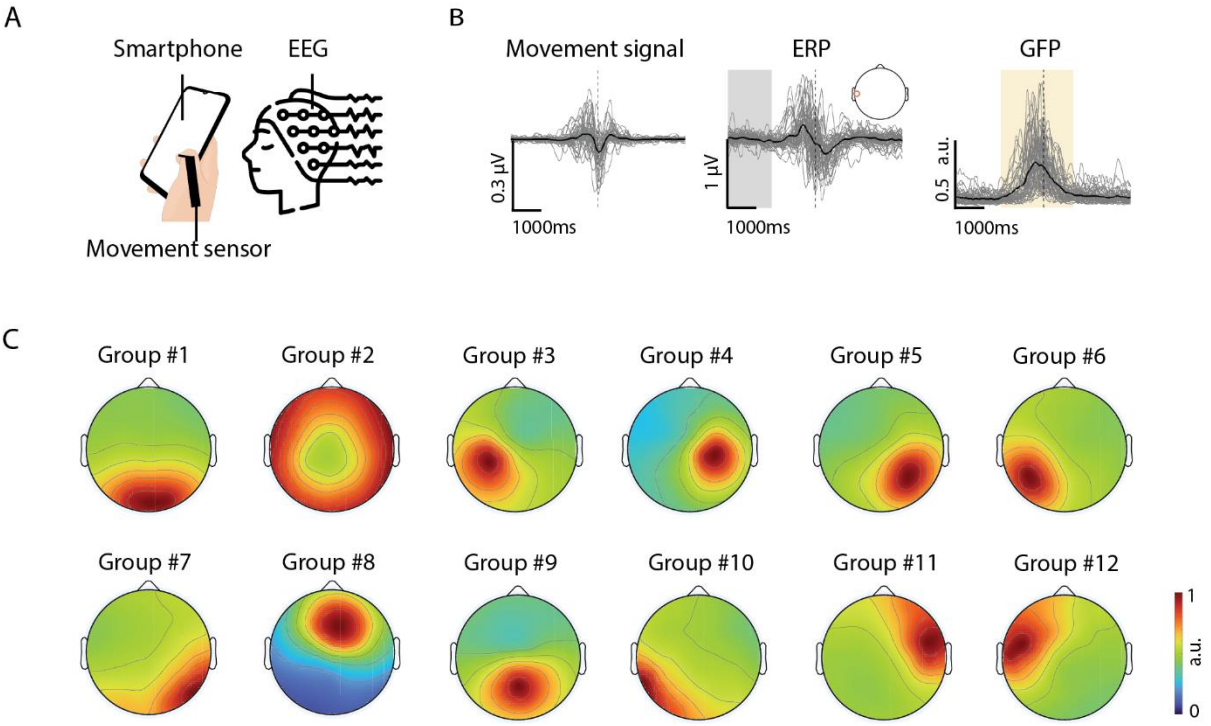

Figure 1. Cortical EEG signals surrounding smartphone touchscreen interactions
(A) Illustration of experimental setup**.** Timestamps of the smartphone touchscreen event were logged by an App on the user's personal smartphone. Right thumb flexion-extension was captured by a movement sensor. Cortical population activity was recorded by using 62 channel scalp EEG. (B) Signals time-locked to smartphone touchscreen interactions. *Left*: black line indicates the grand-averaged (across participants) movement signals time locked to the smartphone interaction (horizontal dashed line). Individual movement traces are shown in grey. *Middle*: The grand-averaged ERP from an electrode placed over the somatosensory cortex (insert) is shown in black while individual ERPs are shown in grey. The analytical baseline period is shaded in grey. *Right*: black line indicates the grand-averaged global field power (GFP) while grey lines indicate individual's GFP. The period of the signal used in the subsequent analysis is shaded in yellow (Time period of interest, TOI). (C) Population-wide averaged EEG independent components based on *k*-means clusters that uses the putative dipole locations (n = 433). We identified 12 clusters, each representing a putatively distinct brain process – the cluster order is preserved throughout the manuscript for cross-referencing.

Delineating cortical processes surrounding smartphone interactions

We simultaneously recorded the smartphone interaction-related movement signals with movement sensor attached to the participants' right thumb and EEG signals. The grand-averaged movement signals indicated an onset of kinematic activity ~ 1 s prior to the smartphone interaction and lasting for another ~ 1 s after the interaction (Fig.1B). Although there were considerable inter-individual differences, there was a consistent downward (towards the screen) pattern of thumb flexion close to the smartphone touchscreen interaction. In the EEG recordings, the electrode placed over the contralateral somatosensory cortex also

showed time-constrained ERP signals (Fig. 1B). To estimate the temporal span of the scalp-wide signals, we used the global field power (GFP), which revealed a period extending from 1424 ms prior to the interaction and 1028 ms thereafter (Fig. 1B). In keeping with prior observations, these patterns indicate that the discrete smartphone touchscreen interactions are surrounded by a delineated period of kinematic and neurophysiological activity (Kock et al., 2023). In the subsequent analysis we focused on this period (Time period of interest, TOI).

We used ICA to separate the putatively distinct brain signal sources. The analysis at the level of each participant revealed ~8 brain sources. To pool information across the population-level, we subsequently grouped these sources (n= 433) according to their putative diploe locations, resulting in 12 typical groups (Fig. 1C), each representing distinct brain processes. The three most prevalent sources were as follows: group#1 (47 participants and 74 ICs, dipoles centered at [5,-79,8] in MNI coordinates, within the occipital cortex, likely corresponding to the visual processing regions), group#2 (35 participant and 41 ICs, dipoles centered at [-3,-21,22], around medial frontal cortex), group#3 (31 participants and 42 ICs, dipoles centered at [-32,-16,59], around left central gyrus, likely involved sensorimotor processing). For the full list of groups see Supplementary Table 1. In sum, a range of putatively distinct signal sources were observed in the period surrounding smartphone interactions implicating distinct cortical processes.

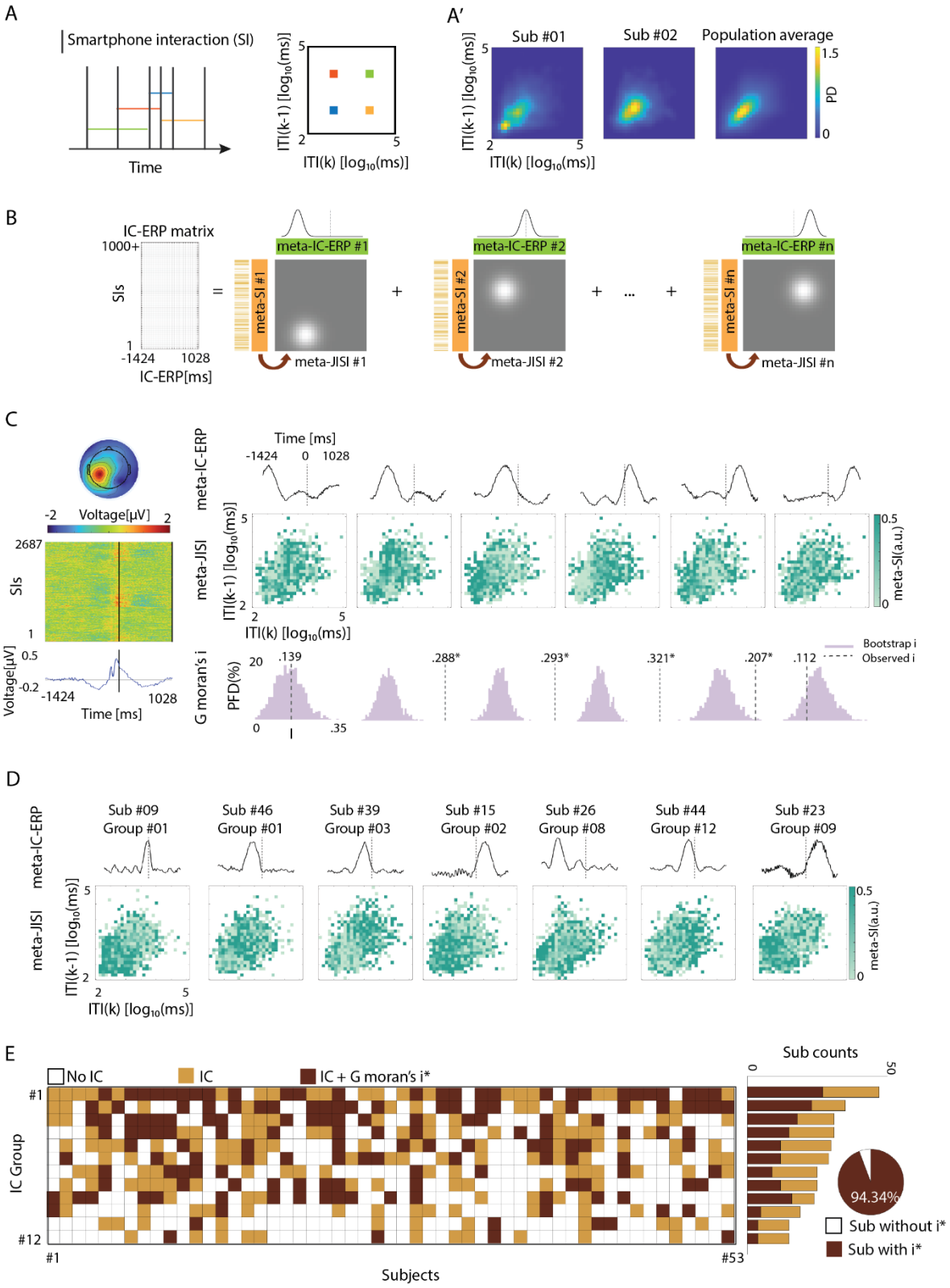

Figure 2. Neuro-behavioral clusters of cortical signals aligned to smartphone next-interval statistics.

A schematic explanation of how next-interval statistics of smartphone touches is captured using the joint interval distribution (JID) approach. (A') The next-interval statistics of smartphone interactions was captured during the EEG measurement session. To illustrate the inter-individual differences, the JID from two participants (Sub#01 and #02) are shown, and averaged JID

stemming from the sampled population (n = 53). (B) Schematic explanation of how we reduced the source-separated cortical signals time-locked to smartphone interactions by using data-driven dimensionality reduction. The source-separated cortical signals were time-locked to the smartphone interactions (SIs) resulting in a signal matrix of interactions number x EEG signal latency. We extracted a lower-rank approximation of the matrix using non-negative matrix factorization (NNMF). The reduced patterns were meta-IC-ERPs – the time-varying neural signal feature – and the corresponding value indicating to what extent the neural feature was present for a given smartphone interaction (meta-SI). The meta-SIs values were then separated according the next-interval statistics of the JID yielding a meta-JISI. (C) Each meta-JISI was tested for 2D temporal auto-correlation. *Top and middle*: For instance, here, the IC cluster #6 of subject 11 was reduced into six neuro-behavioral clusters: meta-IC-ERPs and the corresponding meta-JISIs. *Bottom*: The meta-JISIs were then tested for 2D temporal autocorrelation using Moran's I: an index of how similar the neighborhood is in terms of the meta-JISI values. This value (dashed line) was contrasted to the null distribution of bootstrap shuffled I values – revealing 4 out of 6 meta-JISIs clustered distinctly from the chance levels. (D) Across the population we found a range of clustered neuro-behavioral clusters. These example clusters stem from different subjects and source-separated cortical processes. (E) Overview of the source-separated cortical processes which were found to be clustered in the meta-JISI, i.e., a neural process aligned to the next-interval statistics. Each row depicts a subject and the column depicts the source-separated cortical process. The Brown filled grid indicates a source-separated cortical signal that showed significant 2D temporal autocorrelation and the yellow grid indicates an absence of the same. A white grid indicates the absence of a source-separated process for the corresponding IC group. Bar plots indicate the subject counts with and without the significant autocorrelations. Pie chart indicating the prevalence of significant 2D temporal autocorrelation in the sampled population.

Source-separated cortical signals are aligned to the next-interval smartphone interaction statistics

We captured the next-interval statistics of smartphone interactions using the JID approach (Fig 2A.). Here, the interval (say *k*) is represented along with the previous interval (say *k*-1). While this distribution is well documented in real-world settings, it is new to scenarios where people are asked to use their smartphone during a measurement session in a laboratory. There was considerable variation in the next-interval statistics but short consecutive intervals and interval of similar durations (note, $\log_{10}$ scale) dominated across participants. The interval mostly spanned between ~100 ms and ~10 s. The patterns observed here are in keeping with what is generally observed outside of the laboratory (Ceolini, Kock, et al., 2022).

The distinct source-separated cortical signal surrounding smartphone touchscreen interactions were bridged to the next-interval smartphone statistics by using NNMF and JID analytical framework (Fig. 2B). This analysis was conducted at the level of each individual. Essentially, the matrix of touchscreen interaction-to-interaction variations in EEG signals were reduced to a lower dimensional set of time-varying neural signals (meta-IC-ERP) and a corresponding value indicating the extent of the pattern present for a given interaction (meta-

SI). Separating the meta-SIs according to their corresponding next-interval smartphone interaction statistics revealed clusters of next-interval statistics (meta-JISI), i.e., similar next-interval dynamics shared a common neural signal feature. For instance, in participant # 11, NP # 5, we found a neural signal feature that was prominent ~1 s prior to the interaction and was present in consecutive intervals faster than ~ 1s. In the same cortical process there was another signal which was prominent later (+ 85 ms) and was shared across behaviors slower than ~ 1s. We confirmed these clusters (2D temporal autocorrelations) by using Moran's I and the corresponding bootstrapped null distributions (Fig. 2C).

Across the population, we identified a range of neuro-behavioral clusters (Fig. 2E). Most of the participants (50 out of 53) showed at least one neuro-behavioral cluster with significant 2D temporal autocorrelation. The median number of source-separated cortical processes (IC) group showing one and more neuro-behavior cluster with significant 2D temporal autocorrelation was 3. The top four source-separated cortical processes in terms of showing the behavioral link across the population were located: around occipital cortex (Group #1 , 65.71%,), around posterior cingulate gyrus (Group #2, 57.45%), around frontal cortex (Group #3, 58.06%), and located around the parietal cortex (Group #9, 66.67%). In sum, a range of source-separated cortical signals are shared for behaviors with similar next-interval statistics. Yet the exact cortical source that is aligned and the signal features varies from person to person.

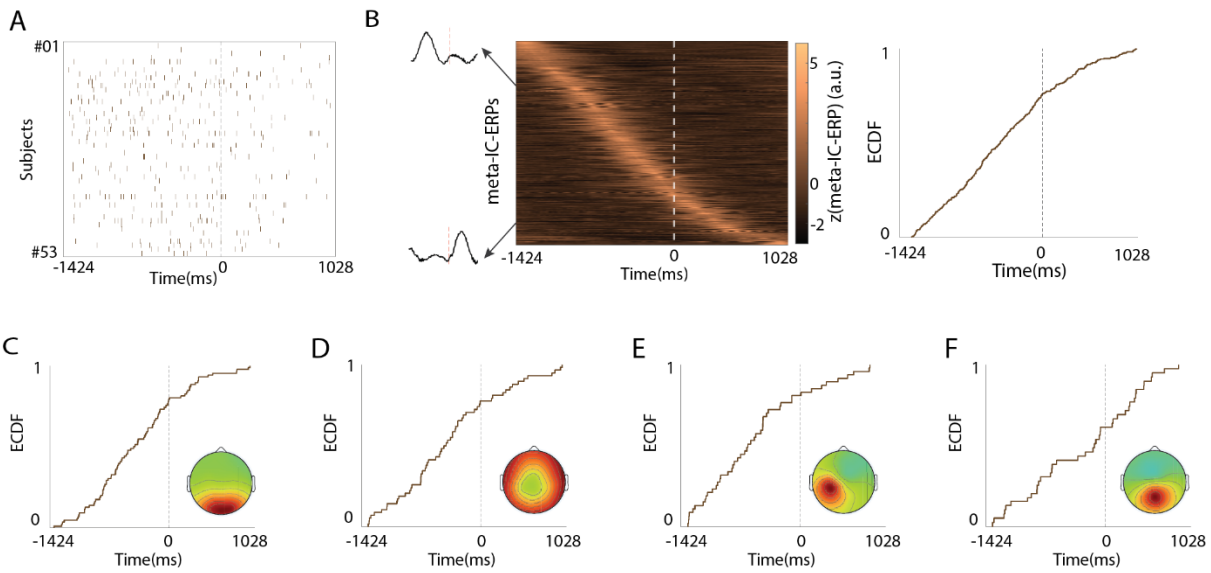

Figure3. Latency of neuro-behavioral clusters relative to smartphone interaction.
(A) The distribution of meta-IC-ERP peak latencies corresponding to all the neuro-behavioral clusters observed in each participant (rows). The distribution is time-locked to the smartphone interaction (dashed line). (B) *Left*: meta-IC-ERPs pooled from all the subjects across all neural processes clusters. The data is sorted according to the peak times. *Right*: The empirical

cumulative distribution function (ECDF) of the peak times. (C-F) The peak times based on meta-IC-ERPs pooled from all the subjects and the four most prevalent clusters (#1 - #3, #9, insert).

The timing of neuro-behavioral clusters relative to the smartphone interaction

The meta-IC-ERP captured the time-variant source-separated cortical signals aligned to the smartphone next-interval statistics. The peak of this signal feature is indicative of the timing when the neuro-behavioral pattern was the most prominent. Therefore, we qualified the peak timings relative to the smartphone interaction for each subject and spanning all the meta-IC-ERPs. At the level of the population, we found that the clustering rate (peak counts/lantency) was 0.0037 (SD=0.0030) prior to the smartphone interaction and 0.0016 (SD=0.0017) after the interaction (Fig. 3). A paired t-test revealed that the clustering rate was significantly higher prior to the interaction than after ($t(52) = 6.1690$, $p = 1.04\times10^{-7}$, 95% CI [0.0014 0.0027]). This pattern of increased neuro-behavioral clustering prior to the interaction was also evident when pooling all the meta-IC-ERPs stemming from all IC groups (Group#1-12). Next, to address whether this pattern was constrained to a specific source-separated cortical signal, we separately examined the meta-IC-ERPs stemming from each IC group. Here the peak-time distributions indicated a pre-interaction prominence for the first three IC clusters. In sum, the neuro-behavioral clustering is more common before the smartphone interaction than after - and this property extends to multiple source-separated neural signals.

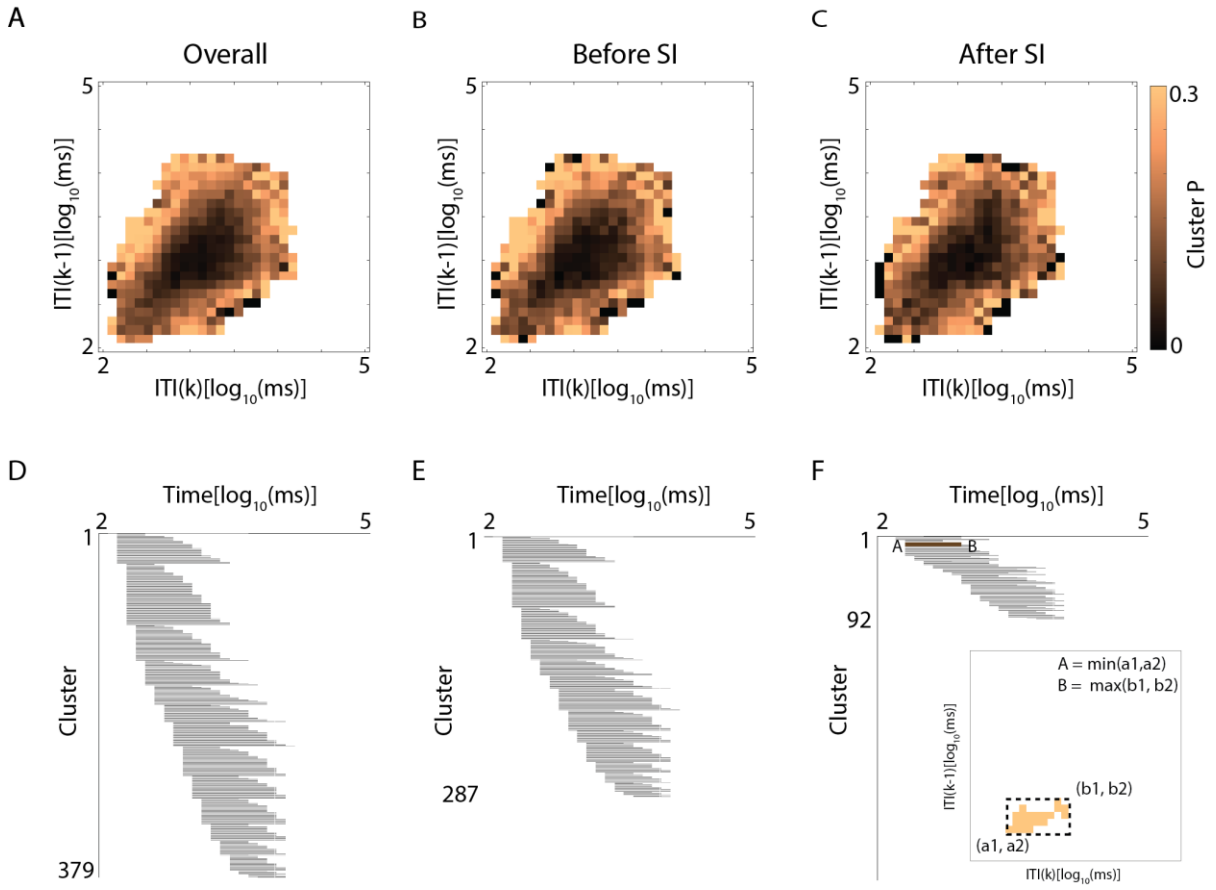

Figure. 4. Isolating the behaviors that are aligned to smartphone next-interval statistics

(A) Binary meta-JISIs were pooled from all participants across all IC clusters. In this pooled set, we estimated the probability of any two-dimensional bin contributing to a cluster according local Moran's I (I > 0.3). (B-C) Same as (A) except that the binary meta-JISIs with corresponding meta-IC-ERP peaks before (B) or after (C) smartphone interaction (SI) was pooled. (D) Time-scale spans of all clusters across all binary meta-JISIs. Each grey line represents the time-scale span of a single cluster. Clusters were included if they contained more than four two-dimensional bins; the span was defined by the minimum and maximum time-scale values of each cluster. (E–F) Same as (D), but clusters were grouped based on whether the corresponding meta-IC-ERP peaks occurred before (E) or after (F) SI.

The smartphone interaction next-interval statistic which contribute to the neuro-behavioral clusters

The meta-JISI of the neuro-behavioral clusters offers an opportunity to gain insight into the nature of the underlying behaviors. To address this, we applied local Moran's I, which identified locations within the meta-JISI exhibiting moderate or higher 2D temporal autocorrelation with their neighbors. We then binarized the local Moran's I matrix by assigning a value of 1 to elements with local Moran's I ⩾ 0.3 and 0 otherwise. In total, 366 binary local Moran's I maps were obtained from 53 participants across all source-separated neural processes. For each two-dimensional bin of the JID, we averaged the corresponding

binary local Moran's I values (Fig. 4A). This analysis revealed that intermediate consecutive intervals were least likely to be spatially clustered, forming a donut-like pattern. Notably, this pattern remained when separating distinct neural processes before and after interaction (Fig. 4B&C).

Finally, we addressed the behavioral temporal span of individual neuro-behavioral clusters. As we were interested in how many time-scales a given cluster may occupy, we focused on the largest neuro-behavioral cluster (bins > 4) delineated by local Moran's I at the level of each meta-JISI. These spans varied, ranging from milliseconds to several seconds. In sum, the results inhibited that the individual cluster can span across multiple time-scales.

Discussion

Smartphone touchscreen touches were accompanied by a complex summation of cortical signals recorded from the scalp. We separated the putatively distinct cortical sources by leveraging the 62 electrodes distributed across the scalp (ICA). These cortical signals varied from one smartphone interaction to the next. By using data-driven dimensionality reduction (NNMF), we extracted neuro-behavioral clusters, revealing the prototypical cortical neural signal features, and the corresponding smartphone touchscreen next-interval statistics. These low-dimensional clusters revealed that similar next-interval statistics of smartphone interaction shared common cortical signal features. Our findings extend the understanding of cortical processes underlying real-world behavior captured on the smartphone.

The neuro-behavioral clusters discovered here are in line with the idea that cortical activity is shaped by the temporal pattern of smartphone behavior. According to carefully designed tasks, comparing slow vs. fast behaviors yields a rough separation of cortical processes serving the sub-second vs. supra-second intervals (Paton & Buonomano, 2018). Our data provides a more fine-grained account where the behaviors are clustered according to their next-interval statistics - and does not indicate a simple separation between slow vs. fast behaviors. Indeed, the absence of simple patterns may stem from an amalgam of intertwined cortical processes from neural inhibition to adaptation (Brands et al., 2024; Chung et al., 2002; David-Jürgens & Dinse, 2010; Garrido et al., 2009; Groen et al., 2022; Huk et al., 2018). Another related idea tied to laboratory tasks is that the brain compares consecutive stimuli and statistical regularities can shape neural information processing (Bengtsson et al., 2004; de Lafuente et al., 2024; Garrido et al., 2009; Garrido et al., 2013; Lieder et al., 2013; Maheu et al., 2019). In the JID space the identical consecutive intervals are represented along the diagonal, but these two-dimensional bins did not pre-dominantly contribute to the neuro-behavioral clusters. Instead, the diagonal was relatively a weaker contributor to the neuro-behavioral clusters in

contrast to bins further away from the diagonal. This raises the possibility that the brain engages neural processes aligned to temporal statistics especially when deviating from temporal regularity.

The meta-IC-ERPs indicated that the neuro-behavioral clusters occur in transients. Essentially, the dominant time-variant signal feature of meta-IC-ERPs was less than 1 s. These time-constrained transients hint at different stages of neural processing being aligned to the temporal statistics of smartphone behavior. Furthermore, even for the same independent component, the contributing behaviors should substantial variation from one transient to the next. This pattern suggests that the processing of a smartphone interaction involves integrating across different next-interval statistics at the different stages of processing. Furthermore, the touchscreen event offered us a landmark to address whether the pre-interaction stages of neuro-behavioral clusters were systematically different from the post-interaction stages. According to a prior event-related potential study, the pre-interaction stages are dominated by preparatory sensorimotor processes whereas post-interaction stages involve information processing and consolidation (Kock et al., 2023). As the neuro-behavioral clusters were more likely to occur before smartphone interaction than after, we speculate that the preparatory stages of information processing leverage the recent temporal statistics to guide the ongoing behavior, whereas the subsequent information processing may reflect the brain automatically integrating the current temporal information into the next-interval statistic system.

While our method provide a coarse isolation of neural signal sources, it did hint at the alignment of distinct cortical processes to the smartphone next-interval statistics. By using independent component analysis, we isolated 12 different sources-separated brain processes groups across the population, of these some were more likely to display neuro-behavioral clusters than others. Components with activity over the frontal, parietal, occipital and temporal cortices, were commonly engaged. These results support the idea that temporal structure underlying naturalistic behavior is encoded by distributed cortex using the patterns of activity of a population of neurons (Buonomano & Laje, 2010; Karmarkar & Buonomano, 2007; Paton & Buonomano, 2018). This cortex-wide tuning to next-interval statistics does not rule out the presence of specialized neural circuits for tracking time. For instance, the secondary somatosensory cortex has been previously implicated in tracking tactile temporal patterns, and it may distribute this information to the rest of the cortex (Rossi-Pool et al., 2021). However, if such a distribution alone was in use, then the same behavioral clusters would reoccur across the source-separated signals - which was not observed.

The patterns discovered here underscore the complexity underlying the cortical processing of real-world behavior. The complexity was particularly vivid when considering the inter-individual differences. Although we could find similar source-separated EEG signals across the population, the corresponding neuro-behavioral clusters varied from person to person. This could be partly due to the distinct behavioral dynamics expressed during the observation period across individuals. But this does not explain the low probability of neuro-behavioral clusters occupying the next-interval statistics which did overlap across individuals. We speculate that the differences stem from different neural strategies that dependent on prior smartphone experience (Balerna & Ghosh, 2018; Gindrat et al., 2015). It also underscores the importance of individualized analysis to study neuro-behavioral correlates in the real world (Akiti et al., 2022; Levy et al., 2023). This supports an emerging literature showing substantial difference across individuals, spanning from behavior, brain activity, and brain-behavior correlation (Finn et al., 2015; Kanai & Rees, 2011; Ozdemir et al., 2020; Wang & He, 2024; Zocher et al., 2020).

The finding of neuro-behavioral clusters parallels the finding of clustered next-interval dynamics in other domains leveraging the smartphone. In healthy aging, there are clusters of behavioral changes across the smartphone JID (Ceolini, Kock, et al., 2022). Long term recordings reveal multi-day rhythms in clusters of next-interval dynamics (Ceolini & Ghosh, 2023). Cognitive testing shows correlations with clusters of next-interval dynamics too (Ceolini, Kock, et al., 2022). In epilepsy, the behavioral correlates of abnormal neural discharges appear clustered as well (van Nieuw Amerongen et al., 2024). The discovery of neuro-behavioral clusters raises the possibility that shared neural processes may underlie the behavioral clusters observed before. In general, our findings suggest the role of temporal structures in the cortical processing of real-world behavior. Methodologically, the combination of the rich smartphone interactions and EEG sets us on an exciting path to unravel the on-demand orchestration of neural processes in the real world.

Method

Participants

Sixty-four participants (age range: 20-81 years; 40 females) were recruited from a participant pool via agestudy.nl research platform (Ceolini, Kock, et al., 2022). All participants had no neurological or psychiatric health disorders according to a self-reported screening at enrolment. Four participants were excluded due to a change in self-reported health status: they had developed tinnitus, stroke, arthrosis, or psychiatric disorder. All participants provided

written informed consent. This study was approved by the Ethics Committee of Psychology at Leiden University (ERB-reference number: 2020-02-14-Ghosh, dr. A.-V2-2044).

Smartphone data collection and joint-interval distribution (JID)

Smartphone behavior was recorded via the TapCounter app (QuantActions AG, Switzerland) (Balerna & Ghosh, 2018). All participants accumulated at least one month of smartphone data before EEG measurement. The app logged each interaction's timestamp in UTC milliseconds in the background. Participants with a ‘does work well’ app status on the EEG measurement day proceeded. During EEG recording, participants freely used one of their four most-used apps from the past month, switched apps every 10 min after a short break. They were asked to use only their right thumb to touch the screen during measurement. Two experimenters monitored participants via live stream in the monitor room and reminded them ‘right thumb only’ when necessary. Participants uploaded their smartphone data via the app after EEG measurement. Two participants were excluded because of missing smartphone data during EEG measurement for unknown reasons.

Interval between smartphone interactions were then calculated, ranging from hundreds of milliseconds to a few seconds. The rich and continuous smartphone behavior can be separated according to the next-interval dynamics using the joint-interval distribution (JID) approach (see Fig. 2A). In brief, we established a two-dimensional space where the x-axis represents the pre-interval (say K) while the y-axis represents the penultimate interval (say K-1) in a logarithmic scale spanning from 100 ms to 10 s. We further binned the space into 30 units along the x-axis and y-axis, respectively, resulting in 900 two-dimensional pixels. Each bin has its own the next-interval properties.

Movement recording and time alignment

Thumb movement was captured using a movement sensor (Flex Sensor, 112 mm, Digi-Key, Thief River Falls). The sensor was attached to participants’ right thumb's dorsum using a custom-made jacket that allowed bending without pulling. Participant were able to freely move their right thumb to interact with smartphone under this setup. Analog signals from the movement sensor were sampled at 1 kHz by using a Polybox (Brain Products GmbH, Gilching, Germany) that fed into a digitizer running on the same clock as used for the EEG signals (see below). Movement signals were processed as described before (Kock et al., 2023). Briefly, the continuous movement signal was band-pass filtered between 1 and 10 Hz and then epoched using a 6 s window centered surrounding each interaction and averaged movement signals across trials for each participant. Then we obtained the grand-averaged movement signals across participants.

However, the smartphone clock may systematically differ from the laboratory clock. To correct for clock differences, we aligned the data using a pre-trained model that estimates the touch times based on the movement sensor signal (Kock et al., 2023). Four participants were excluded due to poor model performance as confirmed by the average movement sensor signal trace. Since movement and EEG data share the same laboratory clock, we corrected the delay between the smartphone-recorded and movement signal predicted interactions. For participants with multiple recording sessions, the predicted interaction time may differ between the sessions due to subtle kinematic differences impacting the movement profile. We utilized *alignsignals* function with xcorr method to align the movement waveforms (Matlab's Signal processing toolbox, MathWorks, Natick, MA, USA). We then calculated the correlation afterward between between these time corrected datasets using Person correlation. Datasets with a correlation value below 0.71 were excluded from further analysis. This threshold was determined using the elbow method based on the empirical cumulative distribution of correlation values across participants.

EEG recording and preprocessing

EEG data were collected using a 64-channels active EEG cap (62 scalp electrodes, 2 ocular electrodes) with a customized equidistant layout (ActiCap Snap, EasyCap Gmbh, Wörthsee, Germany). The EEG signals from the active cap system were referenced to the vertex and amplified with a BrainAmp amplifier (Brain Products GmbH, Gilching, Germany), and digitized at a 1 kHz sampling rate. Participants arrived with clean, washed hair and scalp. The scalp contact sites were further degreased using alcohol swabs. Supervisc gel (Easycap GmbH, Herrsching, Germany) was applied to electrically bridge the skin to the electrode, with electrode impedance targeted below 10 kΩ. The data was processed using the EEGLAB toolbox (Delorme and Makeig, 2004), signal processing toolbox (MATLAB, Mathworks, Natick) and custom scripts in MATLAB 2023b (MATLAB, Mathworks, Natick). The raw data was high-pass filtered at 0.5 Hz. Inactive smartphone use data segments (pre-interval & post-interval >60 s, for instance resulting from checking in with the participant or offering a drink break) were removed from the analysis.

At the individual level averaged ERPs were computed after low-pass filtering at 20 Hz and removing of the artefacts based on ICA results when over 80% likelihood originating from artifacts like blinks, muscles, etc., as evaluated by ICLabel toolbox (Pion-Tonachini et al., 2019). Cleaned EEG data were then epoched from - 3 to 3 s relative to smartphone interaction time. Baseline correction was performed by subtracting the signal mean from -3 to -1.5 s. Grand-averaged ERP signals were then calculated.

To identify the time period of interest (TOI) of event-evoked potentials, we utilized the global field power (GFP), which is a time-variant reference independent indicator of activity based on all of the electrodes (Lehmann & Skrandies, 1980). Here, for each individual, we calculated the averaged ERP for each electrode across trials after trimming extreme value with trimean function. Next, we calculated the standard deviation of ERP across channels at each timepoint (from -3s to 3s with 1ms step). Then, we obtained the grand-averaged GFP (z-transformed) by averaging across participants. To identify the change points of the grand-averaged GFP wave, we utilized *findchangepts* function with the standard division statistic method and a maximum of two change points (Matlab's Signal processing toolbox, MathWorks, Natick). The period between these two change points, -1424 and 1048 ms, were defined as the TOI. The IC-ERPs matrix (see below) was limited to this window for subsequent analysis.

Identifying brain signal sources

We decomposed diverse neural signals on the continuous and pre-processed EEG data by adaptive mixture independent component analysis (AMICA, Palmer et al., 2012; Palmer et al., 2008) with 2,000 maximum iterations. We estimated the equivalent current dipoles and residual variance for each independent component (IC) using DIPFIT toolbox (Delorme et al., 2011). ICs with dipole location out of brain and residual variance over 15% were excluded. We further excluded ICs with less than 50% likelihood originating from brain source, as evaluated by ICLabel toolbox (Pion-Tonachini et al., 2019). One participant was excluded due to no surviving IC after screening. Then, the remaining ICs (n=433) from 53 participants were clustered using *Kmeans* method based on equivalent dipole locations. We explored cluster ranks from 3 to 40, and evaluated the optimal cluster rank using *evalclusters* funtion with 'Silhouette' method implemented in MATLAB. Given the variability introduced by random initialization, we repeated this evaluation procedure 100 times and identified the most frequently selected cluster rank as the final optimal cluster rank. To get a reproducible reduction output using the optimal rank approach, we conducted 1,000 repetitions, each with 10,000 maximum iterations. The final reduction results were selected from the repetition with the best sum of squared distance. Source-separated independent component ERP (IC-ERP) matrix was then reconstructed using *eeg_getdatact (*EEGLAB toolbox*,* Delorme and Makeig, 2004*)* based on the cleaned epoched EEG data with the window of TOI, resulting in a rich neural signals matrix of C (components) $\times$ T (latencies) $\times$ I (smartphone interactions) for each participant.

Identifying neuro-behavioral clusters

For any source-separated cortical signal (for instance, Fig. 2C), there was substantial variation from one smartphone interaction to the next, and this was captured in a neural signal matrix

organized as the no. of interactions x TOI. We extracted the patterns distributed in this rich matrix by using data-driven dimensionality reduction: non-negative matrix factorization (NNMF, Lee and Seung, 1999), which can yield time-varying neural features (*meta-IC-ERP*) that occur at different levels across smartphone interactions (*meta-SI*). This method is detailed elsewhere (Ceolini & Ghosh, 2023). In brief, we obtained a non-negative IC-ERP matrix by subtracting the minimum IC-ERP value from the whole matrix. Next, for each participant and source-separated cortical process, we applied the NNMF to the matrix and searched the optimal cluster ranks (k) between 2 to 15 clusters with 100 repetitions. We identified the optimal k which has the minimum error between the real matrix and the reconstructed matrix. Then, with optimal k identified, we obtained stable and reproducible decomposition by starNNMF with 1000 repetitions. Next, the *meta-SI*, was analyzed in the context of next-interval statistics to reveal how distinct neural processes, activated at specific latencies, map onto the smartphone temporal patterns captured using the JID. For each pixel, we calculated the median value of meta-SIs and yielding a meta-JISI representation.

To assess whether the distribution of meta-JISI was randomly patterned or showed two-dimensional autocorrelations, we adopted the global Moran's I (Moran, 1950). This autocorrelation method is typically utilized to identify spatial autocorrelations but the underlying math can be applied to any two-dimensional representation and capture the similarity a value with its neighborhood (Moran, 1950). In brief, we calculated the global Moran's I for the meta-JISI and a null distribution of Is based on shuffled ordered trials (1000 permutations). One sample t-test (α=0.05) was conducted to compare the real vs. the bootstrapped Is. The neuro-behavioral clusters with distinct I from the null distribution was extracted for further analysis. In a related analysis, we localized the two-dimensional bins participating in the autocorrelations by using local Moran's I (Li et al., 2007).

To address the timing of the neuro-behavioral clusters, we explored the distribution of meta-IC-ERP peak latencies. We contrasted the clustering rate before ($\frac{no.\ of\ peaks}{pre-interaction\ TOI}$) and after ($\frac{no.\ of\ peaks}{post-interaction\ TOI}$) the touchscreen interaction by using a paired t-test. Furthermore, we estimated the empirical cumulative distribution function (eCDF) of the peak latencies for each of the common source-separated cortical processes pooled across individuals.

The meta-JISI of the neuro-behavioural clusters offers an opportunity to gain insight into the nature of the underlying behaviours. To explore this, we applied local Moran's I to identify bins within the meta-JISI showing moderate or higher spatial autocorrelation with neighboring bins (local moran's I >0.3). We then binarized the local Moran's I matrix by assigning 1 to local Moran's I ≥ 0.3 and 0 otherwise. We then averaged these binary values for each two-

dimensional bin of the JID. The same analysis was performed separately for meta-JISI that occurred before and after smartphone interaction. We further examined the time-scale spans of individual neuro-behavioral clusters. Using *bwconncomp* in MATLAB, we identified clusters from all binary meta-JISI and focused on the largest cluster (> 4 bins). This threshold was determined using the elbow method based on the distribution of pooled cluster sizes. For each cluster, we estimated the time-scale span by extracting the minimum and maximum coordinates of its constituent bins. The same analysis was also performed separately for cluster occurred before and after smartphone interaction.

Data, Materials, and Software Availability

The data will be available on dataverse.nl upon publication. The custom-written scripts used towards this report are shared on: https://github.com/CODELABCODELIB/JID_ERP_Smartphone_2024.

Acknowledgements

This project was funded by Velux Stiftung (Grant No.1283, awarded to A.G. with Richard Ridderinkhof as co-applicant). We acknowledge Beste Yavuz, Lysanne Groenewegen, Barbora Michalidesová, Lorenzo Van Hoorde for their help with EEG data collection. We also thank all participants for contributing their time and effort.

Author contributions

A.G. conceived the study. A.G. and W.W. designed the study. W.W acquired, performed EEG pre-processing and analyzed the data with the aid of A.G.. W.W drafted with the aid of A.G.. A.G., W.W. edited the manuscript.

Declaration of interests

A.G. is a co-founder and chairman of QuantActions AG, and is an advisor for Axite B.V. W.W. declares no competing interests.

Reference

Akiti, K., Tsutsui-Kimura, I., Xie, Y., Mathis, A., Markowitz, J. E., Anyoha, R., Datta, S. R., Mathis, M. W., Uchida, N., & Watabe-Uchida, M. (2022). Striatal dopamine explains novelty-induced behavioral dynamics and individual variability in threat prediction. *Neuron*, *110*(22), 3789-3804. e3789.

Balerna, M., & Ghosh, A. (2018). The details of past actions on a smartphone touchscreen are reflected by intrinsic sensorimotor dynamics. *NPJ Digit Med*, *1*, 4. https://doi.org/10.1038/s41746-017-0011-3

Bengtsson, S. L., Ehrsson, H. H., Forssberg, H., & Ullén, F. (2004). Dissociating brain regions controlling the temporal and ordinal structure of learned movement sequences. *European Journal of Neuroscience*, *19*(9), 2591-2602.

Box-Steffensmeier, J. M., Burgess, J., Corbetta, M., Crawford, K., Duflo, E., Fogarty, L., Gopnik, A., Hanafi, S., Herrero, M., Hong, Y. Y., Kameyama, Y., Lee, T. M. C., Leung, G. M., Nagin, D. S., Nobre, A. C., Nordentoft, M., Okbay, A., Perfors, A., Rival, L. M., . . . Wagner, C. (2022). The future of human behaviour research. *Nat Hum Behav*, *6*(1), 15-24. https://doi.org/10.1038/s41562-021-01275-6

Brands, A. M., Devore, S., Devinsky, O., Doyle, W., Flinker, A., Friedman, D., Dugan, P., Winawer, J., & Groen, I. I. A. (2024). Temporal dynamics of short-term neural adaptation across human visual cortex. *PLoS computational biology*, *20*(5), e1012161.

Bueti, D., Lasaponara, S., Cercignani, M., & Macaluso, E. (2012). Learning about time: plastic changes and interindividual brain differences. *Neuron*, *75*(4), 725-737.

Buonomano, D. V., & Laje, R. (2010). Population clocks: motor timing with neural dynamics. *Trends in cognitive sciences*, *14*(12), 520-527.

Ceolini, E., Brunner, I., Bunschoten, J., Majoie, M. H., Thijs, R. D., & Ghosh, A. (2022). A model of healthy aging based on smartphone interactions reveals advanced behavioral age in neurological disease. *IScience*, *25*(8).

Ceolini, E., & Ghosh, A. (2023). Common multi-day rhythms in smartphone behavior. *NPJ Digit Med*, *6*(1), 49. https://doi.org/10.1038/s41746-023-00799-7

Ceolini, E., Kock, R., Band, G. P., Stoet, G., & Ghosh, A. (2022). Temporal clusters of age-related behavioral alterations captured in smartphone touchscreen interactions. *IScience*, *25*(8).

Ceolini, E., Ridderinkhof, K. R., & Ghosh, A. (2024). Age-related behavioral resilience in smartphone touchscreen interaction dynamics. *Proc Natl Acad Sci U S A*, *121*(25), e2311865121. https://doi.org/10.1073/pnas.2311865121

Chung, S., Li, X., & Nelson, S. B. (2002). Short-term depression at thalamocortical synapses contributes to rapid adaptation of cortical sensory responses in vivo. *Neuron*, *34*(3), 437-446.

Cisek, P., & Green, A. M. (2024). Toward a neuroscience of natural behavior. *Curr Opin Neurobiol*, *86*, 102859. https://doi.org/10.1016/j.conb.2024.102859

David-Jürgens, M., & Dinse, H. R. (2010). Effects of aging on paired-pulse behavior of rat somatosensory cortical neurons. *Cerebral Cortex*, *20*(5), 1208-1216.

de Lafuente, V., Jazayeri, M., Merchant, H., García-Garibay, O., Cadena-Valencia, J., & Malagón, A. M. (2024). Keeping time and rhythm by internal simulation of sensory stimuli and behavioral actions. *Science Advances*, *10*(2), eadh8185.

Delorme, A., & Makeig, S. (2004). EEGLAB: an open source toolbox for analysis of single-trial EEG dynamics including independent component analysis. *Journal of neuroscience methods*, *134*(1), 9-21.

Delorme, A., Mullen, T., Kothe, C., Acar, Z. A., Bigdely-Shamlo, N., Vankov, A., & Makeig, S. (2011). Research Article EEGLAB, SIFT, NFT, BCILAB, and ERICA: New Tools for Advanced EEG Processing.

Duckrow, R. B., Ceolini, E., Zaveri, H. P., Brooks, C., & Ghosh, A. (2021). Artificial neural network trained on smartphone behavior can trace epileptiform activity in epilepsy. *IScience*, *24*(6).

Finn, E. S., Shen, X., Scheinost, D., Rosenberg, M. D., Huang, J., Chun, M. M., Papademetris, X., & Constable, R. T. (2015). Functional connectome fingerprinting: identifying individuals using patterns of brain connectivity. *Nature neuroscience*, *18*(11), 1664-1671.

Garrido, M. I., Kilner, J. M., Kiebel, S. J., Stephan, K. E., Baldeweg, T., & Friston, K. J. (2009). Repetition suppression and plasticity in the human brain. *Neuroimage*, *48*(1), 269-279.

Garrido, M. I., Sahani, M., & Dolan, R. J. (2013). Outlier responses reflect sensitivity to statistical structure in the human brain. *PLoS computational biology*, *9*(3), e1002999.

Gindrat, A. D., Chytiris, M., Balerna, M., Rouiller, E. M., & Ghosh, A. (2015). Use-dependent cortical processing from fingertips in touchscreen phone users. *Curr Biol*, *25*(1), 109-116. https://doi.org/10.1016/j.cub.2014.11.026

Goel, A., & Buonomano, D. V. (2014). Timing as an intrinsic property of neural networks: evidence from in vivo and in vitro experiments. *Philosophical transactions of the Royal Society B: Biological sciences*, *369*(1637), 20120460.

Groen, I. I., Piantoni, G., Montenegro, S., Flinker, A., Devore, S., Devinsky, O., Doyle, W., Dugan, P., Friedman, D., & Ramsey, N. F. (2022). Temporal dynamics of neural responses in human visual cortex. *Journal of Neuroscience*, *42*(40), 7562-7580.

Hernández, A., Nácher, V., Luna, R., Zainos, A., Lemus, L., Alvarez, M., Vázquez, Y., Camarillo, L., & Romo, R. (2010). Decoding a perceptual decision process across cortex. *Neuron*, *66*(2), 300-314.

Huk, A., Bonnen, K., & He, B. J. (2018). Beyond trial-based paradigms: Continuous behavior, ongoing neural activity, and natural stimuli. *Journal of Neuroscience*, *38*(35), 7551-7558.

Kanai, R., & Rees, G. (2011). The structural basis of inter-individual differences in human behaviour and cognition. *Nature Reviews Neuroscience*, *12*(4), 231-242.

Karmarkar, U. R., & Buonomano, D. V. (2007). Timing in the absence of clocks: encoding time in neural network states. *Neuron*, *53*(3), 427-438.

Koch, G., Oliveri, M., & Caltagirone, C. (2009). Neural networks engaged in milliseconds and seconds time processing: evidence from transcranial magnetic stimulation and patients with cortical or subcortical dysfunction. *Philos Trans R Soc Lond B Biol Sci*, *364*(1525), 1907-1918. https://doi.org/10.1098/rstb.2009.0018

Kock, R., Ceolini, E., Groenewegen, L., & Ghosh, A. (2023). Neural processing of goal and non-goal-directed movements on the smartphone. *Neuroimage: Reports*, *3*(2), 100164.

Kock, R., & Ghosh, A. (2024). Neural microstates in real-world behaviour captured on the smartphone. *bioRxiv*, 2024.2007. 2022.604605.

Krakauer, J. W., Ghazanfar, A. A., Gomez-Marin, A., MacIver, M. A., & Poeppel, D. (2017). Neuroscience Needs Behavior: Correcting a Reductionist Bias. *Neuron*, *93*(3), 480-490. https://doi.org/10.1016/j.neuron.2016.12.041

Lee, D. D., & Seung, H. S. (1999). Learning the parts of objects by non-negative matrix factorization. *nature*, *401*(6755), 788-791.

Lehmann, D., & Skrandies, W. (1980). Reference-free identification of components of checkerboard-evoked multichannel potential fields. *Electroencephalography and clinical neurophysiology*, *48*(6), 609-621.

Levy, D. R., Hunter, N., Lin, S., Robinson, E. M., Gillis, W., Conlin, E. B., Anyoha, R., Shansky, R. M., & Datta, S. R. (2023). Mouse spontaneous behavior reflects individual variation rather than estrous state. *Current Biology*, *33*(7), 1358-1364. e1354.

Lewis, P. A., & Miall, R. C. (2003). Brain activation patterns during measurement of sub- and supra-second intervals. *Neuropsychologia*, *41*(12), 1583-1592. https://doi.org/10.1016/s0028-3932(03)00118-0

Li, H., Calder, C. A., & Cressie, N. (2007). Beyond Moran's I: testing for spatial dependence based on the spatial autoregressive model. *Geographical analysis*, *39*(4), 357-375.

Lieder, F., Daunizeau, J., Garrido, M. I., Friston, K. J., & Stephan, K. E. (2013). Modelling trial-by-trial changes in the mismatch negativity. *PLoS computational biology*, *9*(2), e1002911.

Liu, J. K., Schreyer, H. M., Onken, A., Rozenblit, F., Khani, M. H., Krishnamoorthy, V., Panzeri, S., & Gollisch, T. (2017). Inference of neuronal functional circuitry with spike-triggered non-negative matrix factorization. *Nature communications*, *8*(1), 149.

Lu, N., & Yin, T. (2015). Motor imagery classification via combinatory decomposition of ERP and ERSP using sparse nonnegative matrix factorization. *Journal of neuroscience methods*, *249*, 41-49.

Machens, C. K., Romo, R., & Brody, C. D. (2005). Flexible control of mutual inhibition: a neural model of two-interval discrimination. *Science*, *307*(5712), 1121-1124.

Maheu, M., Dehaene, S., & Meyniel, F. (2019). Brain signatures of a multiscale process of sequence learning in humans. *elife*, *8*, e41541.

Martin, C. B., Hong, B., Newsome, R. N., Savel, K., Meade, M. E., Xia, A., Honey, C. J., & Barense, M. D. (2022). A smartphone intervention that enhances real-world memory and promotes differentiation of hippocampal activity in older adults. *Proceedings of the National Academy of Sciences*, *119*(51), e2214285119.

Miller, C. T., Gire, D., Hoke, K., Huk, A. C., Kelley, D., Leopold, D. A., Smear, M. C., Theunissen, F., Yartsev, M., & Niell, C. M. (2022). Natural behavior is the language of the brain. *Current Biology*, *32*(10), R482-R493.

Moran, P. A. (1950). Notes on continuous stochastic phenomena. *Biometrika*, *37*(1/2), 17-23.

Onton, J., Westerfield, M., Townsend, J., & Makeig, S. (2006). Imaging human EEG dynamics using independent component analysis. *Neuroscience & Biobehavioral Reviews*, *30*(6), 808-822.

Ozdemir, R. A., Tadayon, E., Boucher, P., Momi, D., Karakhanyan, K. A., Fox, M. D., Halko, M. A., Pascual-Leone, A., Shafi, M. M., & Santarnecchi, E. (2020). Individualized perturbation of

the human connectome reveals reproducible biomarkers of network dynamics relevant to cognition. *Proceedings of the National Academy of Sciences*, *117*(14), 8115-8125.

Palmer, J. A., Kreutz-Delgado, K., & Makeig, S. (2012). AMICA: An adaptive mixture of independent component analyzers with shared components. *Swartz Center for Computatonal Neursoscience, University of California San Diego, Tech. Rep*, 1-15.

Palmer, J. A., Makeig, S., Kreutz-Delgado, K., & Rao, B. D. (2008). Newton method for the ICA mixture model. 2008 IEEE International Conference on acoustics, speech and signal processing,

Paton, J. J., & Buonomano, D. V. (2018). The neural basis of timing: distributed mechanisms for diverse functions. *Neuron*, *98*(4), 687-705.

Petter, E. A., Lusk, N. A., Hesslow, G., & Meck, W. H. (2016). Interactive roles of the cerebellum and striatum in sub-second and supra-second timing: Support for an initiation, continuation, adjustment, and termination (ICAT) model of temporal processing. *Neuroscience & Biobehavioral Reviews*, *71*, 739-755.

Pfister, J.-P., & Ghosh, A. (2020). Generalized priority-based model for smartphone screen touches. *Physical Review E*, *102*(1), 012307.

Pion-Tonachini, L., Kreutz-Delgado, K., & Makeig, S. (2019). ICLabel: An automated electroencephalographic independent component classifier, dataset, and website. *Neuroimage*, *198*, 181-197.

Rossi-Pool, R., Zainos, A., Alvarez, M., Diaz-deLeon, G., & Romo, R. (2021). A continuum of invariant sensory and behavioral-context perceptual coding in secondary somatosensory cortex. *Nature communications*, *12*(1), 2000.

van de Ruit, M., & Ghosh, A. (2022). Can you hear me now? Momentary increase in smartphone usage enhances neural processing of task-irrelevant sound tones. *Neuroimage: Reports*, *2*(4), 100131.

van Nieuw Amerongen, A. R., Meppelink, A. M., Ghosh, A., & Thijs, R. D. (2024). Real - world smartphone data can trace the behavioural impact of epilepsy: A case study. *European Journal of Neurology*, *31*(12), e16433.

Wan, W., Ridderinkhof, K. R., & Ghosh, A. (2024). The timing of preceding tactile inputs modulates cortical processing. *bioRxiv*, 2024.2007. 2022.604577.

Wang, J., & He, Y. (2024). Toward individualized connectomes of brain morphology. *Trends in Neurosciences*, *47*(2), 106-119.

Wessel, J. R., & Aron, A. R. (2017). On the globality of motor suppression: unexpected events and their influence on behavior and cognition. *Neuron*, *93*(2), 259-280.

Wessel, J. R., Jenkinson, N., Brittain, J.-S., Voets, S. H., Aziz, T. Z., & Aron, A. R. (2016). Surprise disrupts cognition via a fronto-basal ganglia suppressive mechanism. *Nature communications*, *7*(1), 11195.

Zocher, S., Schilling, S., Grzyb, A. N., Adusumilli, V. S., Bogado Lopes, J., Günther, S., Overall, R. W., Winter, Y., & Kempermann, G. (2020). Early-life environmental enrichment generates persistent individualized behavior in mice. *Science Advances*, *6*(35), eabb1478.